

Reaction $^{114}\text{Cd}(p, p')$ by use of polarized protons and proton- γ angular correlations

S. Schneider, W. Eyrich, A. Hofmann, U. Scheib, and F. Vogler

Physikalisches Institut, University Erlangen-Nürnberg, Erlangen, Germany

(Received 27 December 1978)

The reactions $^{114}\text{Cd}(p, p')$ and $^{114}\text{Cd}(p, p'\gamma)$ have been studied for polarized and unpolarized protons at a bombarding energy of 11 MeV. Differential and double differential cross sections as well as analyzing powers, correlation asymmetries, and the spin flip probability have been measured by use of a multidetector arrangement consisting of 11 silicon surface barrier detectors and two Ge(Li) detectors. The experimental data have been analyzed in terms of coupled channels on the basis of a harmonic vibrator and a rigid symmetric rotator model. The correlation data are found to be more sensitive to the models used and the sign of the quadrupole deformation than differential cross sections and analyzing powers. Considering the correlation data, the rotator model with oblate deformation must be ruled out for ^{114}Cd . The best description of the experiment is obtained by the harmonic vibrator model. Compound nucleus contributions can be neglected.

NUCLEAR REACTIONS $^{114}\text{Cd}(p, p')$, $^{114}\text{Cd}(p, p'\gamma)$, $E=11$ MeV; polarized and unpolarized protons; measured analyzing powers, inplane $p_1\gamma$ -correlations and spin flip probability. Coupled channels analyses; enriched target.

INTRODUCTION

The theoretical description of a nuclear reaction of the type $A(a, b)B$ in the frame of a direct reaction model is usually performed in terms of transition amplitudes $X_{m_a M_A m_b M_B}$ between the magnetic substates of the entrance and exit channel. In order to test the reaction mechanism, generally the differential cross section, which consists of the sum of the squares of the transition amplitudes, is analyzed. In many cases the knowledge of the differential cross section alone is not sufficient to make a definitive statement about the validity of a reaction model. Therefore, one has to look for additional quantities, which contain other combinations of the transition amplitudes.

Such quantities, which can be expected to test the reaction mechanism in a more sensitive way are, e.g., the analyzing powers, where interference terms relating to the substate m_a occur, and particle- γ angular correlation functions, in which interference terms relating to M_B occur. It has been shown that analyzing power measurements^{1,2} as well as particle- γ angular correlation measurements^{3,4} indeed are suitable to gain more detailed information about the reaction mechanism than the differential cross section.

In the present work we measured the analyzing power and proton- γ angular correlations of inelastic proton scattering from ^{114}Cd in order to investigate whether these quantities are influenced in a different way by the different reaction models and their parameters. Additionally we measured angular correlations using polarized protons. In

this case interference terms relating to both m_a and M_B occur; therefore, this experiment should offer even more insight into the reaction than the analyzing power and the angular correlations with unpolarized projectiles.

There are different nuclear model assignments for ^{114}Cd . The energies and the spin sequence of the lower lying levels suggest the use of a vibrator model; therefore, most of the analyses have been done in this model.⁵⁻⁷ Various properties, however, such as the energy splitting of the two quadrupole phonon triplet, its γ -branching, and the large quadrupole moment of the first 2^+ level cannot be explained satisfactorily within a harmonic vibrator model. Mainly the existence of this large quadrupole moment led to the assumption that ^{114}Cd is a permanently deformed nucleus.⁸ It was a further aim of the present work to show whether a definite statement is possible about the validity of the rotator or vibrator model and the sign of the quadrupole deformation.

EXPERIMENT

The experiments were performed at the correlation beam tube of the Erlangen EN tandem accelerator at a bombarding energy of 11 MeV. The focusing of the beam was controlled permanently by a system of slits, because the beam position had to be constant, especially during all the measurements with polarized particles.

In these experiments we used special properties of the reaction chamber,⁹ which had been designed especially for particle- γ -correlation measure-

ments. For example, in measuring the spin flip probability, the reaction chamber was turned 90° on the beam axis, thereby making simpler the positioning of the γ detector (perpendicular to the reaction plane). As a target we used a self-supporting foil consisting of ^{114}Cd (enrichment $>98.8\%$) with a thickness of 2 mg/cm^2 .

In the measurements with unpolarized protons the current was $30\text{--}40\text{ nA}$, with polarized protons the current was $10\text{--}20\text{ nA}$. The polarized protons were produced by the Erlangen Lamb-shift source¹⁰; the polarization of the beam was monitored by a ^{12}C polarimeter, combined with a Faraday cup. The average polarization was about 70% . The deviation from this value was less than 2% within 60 h .

For the detection of the scattered protons 11 silicon surface barrier detectors were used. The γ radiation was detected by two Ge(Li) detectors having efficiencies of 10% and 8% , respectively. Each of the γ detectors worked in coincidence with all the particle detectors. Figure 1 shows a block diagram of the electronics. The time sig-

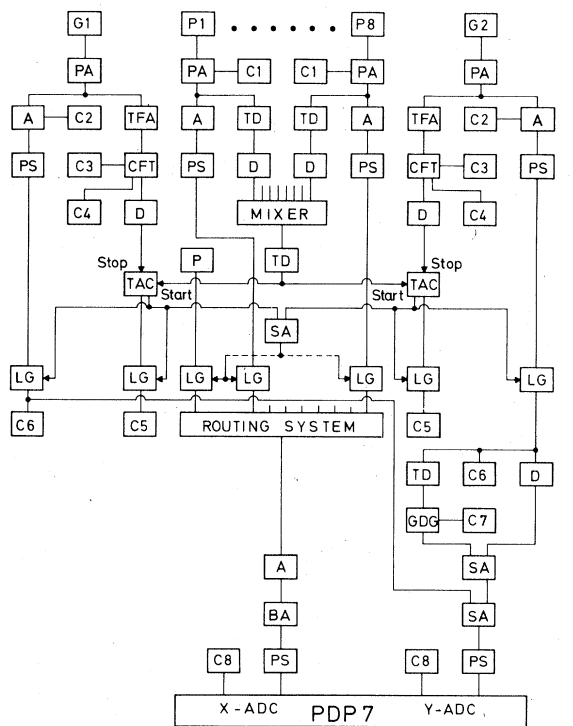


FIG. 1. Block diagram of the electronics, G1, G2 γ detectors, P1-P8 particle detectors, PA preamplifiers, A amplifiers, TFA timing filter amplifiers, TD threshold discriminators, PS pulse stretchers, CFT constant fraction triggers, D delay lines, TAC time analyzers, P pulse generator, SA sum amplifiers, LG linear gates, GDG gate and delay generator, BA biased amplifier, C1-C8 test points.

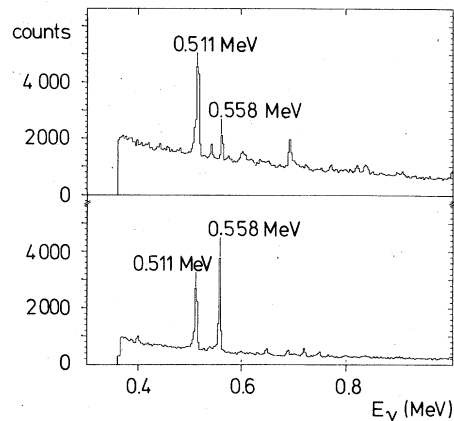


FIG. 2. Upper part: "free" γ spectrum. Lower part: γ spectrum obtained in coincidence with the pulses of all particle detectors.

nals from the preamplifiers, which fulfilled the coincidence requirement, served as enabling signals for the linear gates. The coincident energy pulses of the particle and γ detectors were routed and analyzed by two analog-to-digital converters (ADC's) in conjunction with a PDP-7 on-line computer. The electronics and detectors were monitored at several control points (C1-C8 in Fig. 1). Moreover, the stability of the beam could be controlled by the counting rate of the γ detector (C3). When the beam quality was optimal this counting rate reached a minimum value.

In the upper part of Fig. 2 a "free" γ spectrum of one of the two γ detectors is shown, the lower part shows the corresponding γ spectrum of a coincidence measurement (γ signals in coincidence with all the particle signals). The enhancement of the 558 keV γ peak, which corresponds to the 2^+

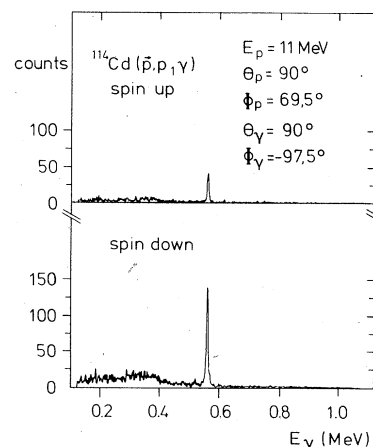


FIG. 3. γ spectrum in coincidence with the p_1 peak of a one particle spectrum. Upper part: spin position "up," lower part: spin position "down."

$\rightarrow 0^+$ transition in ^{114}Cd , can be clearly seen in the coincidence spectrum. It is obvious that a Ge(Li) detector is necessary to separate the 558 keV peak from the 511 keV annihilation quanta.

In Fig. 3 two coincidence γ spectra are shown measured in the reaction plane with opposite direction of the proton spin. The double differential cross sections were obtained by integrating the photopeaks of such spectra. More information about data evaluation and more experimental details are given elsewhere.⁹

THEORY

For the theoretical treatment of particle- γ angular correlations induced by polarized projectiles we adopt the formalism of Debenham and Satchler.¹¹ Consider the nuclear reaction $A(a, b)B$, which is described by the reaction amplitudes $X_{m_a M_A m_b M_B}$ between the magnetic substates of the entrance and exit channel. By the use of polarized projectiles the differential cross section is written as

$$\left. \frac{d\sigma}{d\Omega} \right|_{\text{pol}} = \left. \frac{d\sigma}{d\Omega} \right|_{\text{unpol}} \left(\sum_{kq} T_{kq} t_{kq}^* \right), \quad (1)$$

where the analyzing powers T_{kq} are defined in agreement with the Madison convention¹²:

$$T_{kq} = \frac{\rho^{kq}}{\rho^{00}}$$

$$G_{KQ}^{kq}(\theta_b, \phi_b) = \sum_{m_a m_a' M_A m_b M_B} X_{m_a M_A m_b M_B}(\theta_b, \phi_b) X_{m_a' M_A m_b M_B}^*(\theta_b, \phi_b) (-1)^{s_a - m_a'} (2s_a + 1)^{1/2} \times (s_a s_a m_a - m_a' | kq) (-1)^{J_B - M_B} (J_B J_B M_B - M_B' | KQ). \quad (4)$$

The transfer coefficients G_{KQ}^{kq} are related to the statistical tensors ρ_{KQ} by

$$\rho_{KQ}(J_B) = \sum_{kq} t_{kq}^*(s_a) G_{KQ}^{kq}(\theta_b, \phi_b). \quad (5)$$

From these tensors ρ_{KQ} one obtains the angular correlation function in the well-known form¹³

$$W(\theta_b, \phi_b, \theta_\gamma, \phi_\gamma) = \sum_{KQ} \frac{\rho_{KQ}(J_B)}{\rho_{00}(J_B)} R_K(\gamma) C_{KQ}(\theta_\gamma, \phi_\gamma). \quad (6)$$

The double differential cross section, which is the quantity measured directly in particle- γ correlation measurements, becomes

$$\frac{d^2\sigma}{d\Omega_b d\Omega_\gamma} = \frac{1}{4\pi} \frac{\Gamma_{\gamma C}^B}{\Gamma^B} W(\theta_b, \phi_b, \theta_\gamma, \phi_\gamma) \frac{d\sigma}{d\Omega_b}(\theta_b, \phi_b). \quad (7)$$

($\Gamma_{\gamma C}^B/\Gamma^B$ gives the branching ratio.)

Analogous to the analyzing power T_{10} , the correlation asymmetry CA is introduced by use of the double differential cross sections for the spin position up and down. It is given by

$$\text{CA} = \left(\frac{d^2\sigma \uparrow}{d\Omega_b d\Omega_\gamma} - \frac{d^2\sigma \downarrow}{d\Omega_b d\Omega_\gamma} \right) / \left(\frac{d^2\sigma \uparrow}{d\Omega_b d\Omega_\gamma} + \frac{d^2\sigma \downarrow}{d\Omega_b d\Omega_\gamma} \right) = \frac{\sum_{KQ} G_{KQ}^{10} R_K C_{KQ}}{\sum_{KQ} \rho_{KQ}^{\text{unpol}} R_K C_{KQ}}. \quad (8)$$

Finally, we consider the spin flip probability, which is obtained when unpolarized protons are used in the entrance channel and the coincident γ radiation is detected perpendicular to the reaction plane. For a

and

$$\rho^{kq}(J_B) = (2J_B + 1)^{-1/2} \sum_{m_a m_a' M_A m_b M_B} X_{m_a M_A m_b M_B} \times (\theta_b, \phi_b) X_{m_a' M_A m_b M_B}^*(\theta_b, \phi_b) (-1)^{s_a - m_a'} \times (2s_a + 1)^{1/2} (s_a s_a m_a - m_a' | kq). \quad (2)$$

The analyzing powers T_{kq} include interference terms of reaction amplitudes $X_{m_a M_A m_b M_B}$ relating to the substate m_a . The tensors t_{kq}^* are composed of the density matrix elements of the beam $\rho_{m_a m_a'}$:

$$t_{kq}^*(s_a) = \sum_{m_a m_a'} \rho_{m_a m_a'}(s_a) (-1)^{s_a - m_a'} \times (2s_a + 1)^{-1/2} (s_a s_a m_a - m_a' | kq). \quad (3)$$

With polarized protons in the entrance channel, only the tensors $T_{00} = t_{00} = 1$, T_{10} , and t_{10} occur in Eq. (1). (For the present work the z axis was chosen perpendicular to the reaction plane.) For the spin position "up," t_{10}^* becomes +1, for the spin position "down," $t_{10}^* = -1$. Therefore, the vector analyzing power T_{10} may be extracted by a measurement using both spin positions.

Considering particle- γ correlations with polarized projectiles, the analyzing powers T_{kq} are replaced by the polarization transfer coefficients G_{KQ}^{kq} . They include interference terms of reaction amplitudes relating to the substates m_a and M_B :

transition with the spin sequence ($J_A = 0^+$) \rightarrow ($J_B = 2^+$) \rightarrow ($J_C = 0^+$), only reaction amplitudes $X_{M_B=\pm 1}$ can contribute. The spin flip probability W_S may be written as

$$W_S(\theta_\gamma = 0^\circ) = \frac{5}{4} \frac{1}{d\sigma/d\Omega_b} \left[\sum_{m_a M_A m_b} X_{m_a M_A m_b M_B=+1}(\theta_b \phi_b) X_{m_a M_A m_b M_B=+1}^*(\theta_b \phi_b) + \sum_{m_a M_A m_b} X_{m_a M_A m_b M_B=-1}(\theta_b \phi_b) X_{m_a M_A m_b M_B=-1}^*(\theta_b \phi_b) \right]. \quad (9)$$

ANALYSIS AND DISCUSSION

All the calculations in this work were done in terms of coupled channels (CC) (Ref. 14) on the basis of the harmonic vibrator and the rigid symmetric rotator model, respectively. In addition, the influence of sign and magnitude of the quadrupole deformation on the different quantities to be measured was studied.

First of all we tried to obtain the best possible description of the differential cross sections of the elastic and inelastic proton scattering from ^{114}Cd . In contrast to the analyzing powers the differential cross sections are not as strongly affected by the parameters of the spin orbit potential. Therefore, the parameters for the spin orbit potential are obtained by fitting the experimental analyzing powers of elastic and inelastic scattering. For the spin orbit potential a full Thomas form¹⁵ was used.

The fitting procedure was done with the CC code ECIS76 (Ref. 16) in complex coupling including Coulomb excitation. With the best fitted parameter sets (see Table I) obtained from the analysis of the differential cross sections and the analyzing powers, the double differential cross sections, the correlation asymmetry, and the spin flip probability were calculated with the computer code CWK2.¹⁷

CC ANALYSIS IN 0^+-2^+ COUPLING

At first the calculations were done in a 0^+-2^+ coupling scheme. These results are discussed in the following sections. The upper part of Fig. 4 shows the experimental cross sections for the elastic and inelastic proton scattering measured in the angular region $20^\circ < \phi_{p,c.m.} < 160^\circ$ at a bom-

barding energy of 11 MeV. Within the whole angular region the best fitted CC calculations based on the vibrational model as well as on the rotational model for prolate and oblate deformation, respectively, show very good agreement with the experimental data. (The χ^2 values of the fits corresponding to the different models differ by less than 20%.) The resulting values for the quadrupole deformation (see Table I) are in good agreement with the results of other experiments.¹⁸ The numerical value of β_2 turns out to be larger in the oblate case than in the prolate case. This behavior can also be seen in α -scattering data.¹⁹

The lower part of Fig. 4 shows the experimental analyzing powers T_{10} for the elastic and inelastic scattering for the angular regions $40^\circ < \phi_{p,c.m.} < 160^\circ$ and $70^\circ < \phi_{p,c.m.} < 160^\circ$, respectively. Obviously the experimental values of the analyzing powers are relatively small ($T_{10} < 0.2$) for the whole angular region. This agrees with the results attained by Raynal,²⁰ who found small analyzing powers for nuclei near a closed proton shell and an open neutron shell.

The CC calculations for the elastic analyzing power differ very little for the different reaction models. We find, however, some differences in the various calculations for the inelastic analyzing power; there is a phase shift between the curve corresponding to $\beta_2 > 0$ and the two curves corresponding to $\beta_2 < 0$ and to the vibrational model. In the angular region $80^\circ < \phi_{p,c.m.} < 120^\circ$ the agreement with the experimental data is better for calculations assuming a rotator with $\beta_2 < 0$ or a vibrator; in the remaining angular region the calculation assuming a rotator with $\beta_2 > 0$ shows the closer agreement. [This phase shift in the inelas-

TABLE I. Best fitted parameters of the CC calculations (potential depths in MeV; length in fm).

	V_0	r_0	a_0	W_D	r_D	a_D	V_{SO}	r_{SO}	a_{SO}	r_c	β
VIB (0^+-2^+-C)	59.07	1.14	0.926	13.69	1.33	0.538	4.83	1.30	0.34	1.20	0.164
ROT (0^+-2^+-C ; $\beta > 0$)	54.36	1.20	0.764	9.56	1.25	0.774	6.00	1.20	0.70	1.25	0.172
ROT (0^+-2^+-C ; $\beta < 0$)	55.37	1.20	0.785	11.48	1.25	0.732	6.00	1.20	0.70	1.25	-0.185
VIB (0^+-2^+-C)	63.81	1.10	0.940	13.13	1.31	0.530	4.83	1.30	0.34	1.20	0.171
ROT ($0^+-2^+-4^+-C$; $\beta > 0$)	53.70	1.20	0.830	10.59	1.31	0.640	5.00	1.20	0.70	1.25	0.164
ROT ($0^+-2^+-4^+-C$; $\beta < 0$)	61.67	1.08	1.020	15.06	1.37	0.500	5.00	1.20	0.70	1.35	-0.165

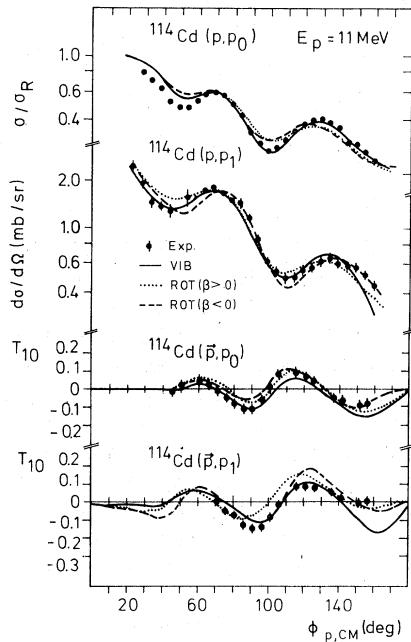


FIG. 4. Experimental differential cross sections and analyzing powers of the reactions $^{114}\text{Cd}(p, p_0)^{114}\text{Cd}$ and $^{114}\text{Cd}(p, p_1)^{114}\text{Cd}$ in comparison with CC best fitted calculations.

tic analyzing power between the dotted curve ($\beta_2 > 0$) and the other ones can be removed by assuming different deformations for the spin orbit and the central part of the optical potential.²¹ On the whole, all three curves are able to describe the experimental analyzing powers in a satisfactory way.

Therefore, it was of interest to see whether this good agreement between experiment and theory can also be found in the correlation data, or whether these correlation data would lead to an even greater sensitivity regarding the different reaction models and the sign of the quadrupole deformation. For this reason we measured the angular distribution of the double differential cross section at several positions of the γ detector in the reaction plane using unpolarized protons in the entrance channel. As an example, in Fig. 5 the results for $\theta_\gamma = 90^\circ$ and $\phi_\gamma = 90^\circ$ is shown and compared to the predictions of the CC theory. (The particle detectors were mounted in the angular region at 60° to 150° .) Very good agreement could be achieved between the CC prediction assuming a vibrational model and the experimental data. The theoretical curves assuming a rotational model show a somewhat different behavior. Only the calculation for $\beta_2 > 0$ is able to reproduce the experimental data in the whole angular region. The same result is also found for the double dif-

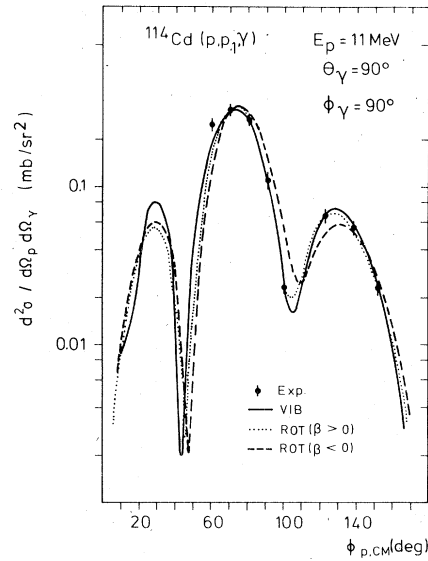


FIG. 5. Experimental double differential cross section of the reaction $^{114}\text{Cd}(p, p_1\gamma)^{114}\text{Cd}$ in comparison with CC predictions in a $0^+ - 2^+$ coupling scheme.

ferential cross sections measured at other positions of the γ detector in the reaction plane. Therefore, the rotational model assuming an oblate deformation for ^{114}Cd can be excluded by the consideration of the double differential cross section.

Moreover, we measured angular correlations using polarized protons. In Fig. 6 an experimental correlation asymmetry is compared to the CC calculations using the best fitted parameter sets. The particle detectors are placed within the angular region 60° to 150° and the γ detector is situated

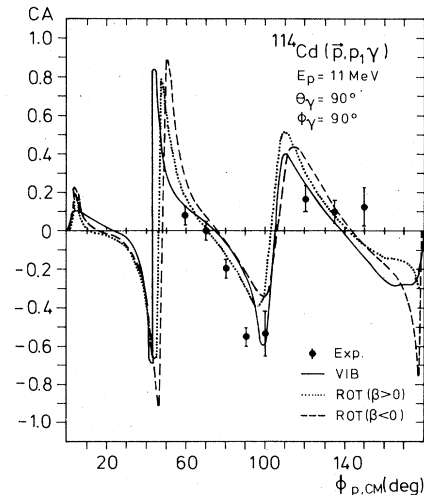


FIG. 6. Experimental correlation asymmetry of the reaction $^{114}\text{Cd}(p, p_1\gamma)^{114}\text{Cd}$ in comparison with CC predictions.

in the reaction plane at 90° . Now in contrast to the "unpolarized" double differential cross sections, more pronounced differences between the different CC predictions occur, especially, between the rotational model for $\beta_2 > 0$ and the vibrational model. The same result is obtained when the correlation asymmetry is measured at other positions of the γ detector. It can be stated that the vibrational model gives the best description of the experimental data. The rotational model gives a worse description of the experimental correlation asymmetry, but cannot be definitively excluded with this data.

SPIN FLIP PROBABILITY AND COMPOUND NUCLEUS CONTRIBUTIONS

The analyses of the present work were done in the framework of direct reaction models. This is justified only if compound nucleus contributions are negligible. Therefore, we proved that this is true for the reaction $^{114}\text{Cd}(p, p')^{114}\text{Cd}$ at the bombarding energy of 11 MeV. For that purpose we measured the spin flip probability, which is known to be very sensitive to compound nuclear contributions.²² Figure 7 shows the experimental spin flip probability together with calculations assuming a pure direct reaction (vibrational model) and a pure compound reaction (Hauser-Feshbach model), respectively. The experimental points are corrected due to the finite aperture of the γ detector, which had an effective angle of ± 7.5 degrees. This correction was done by the method described in Ref. 23. The transmission coefficients for the Hauser-Feshbach calculations, done with the program MANDY,²⁴ were obtained from the optical model parameters of the vibrational model

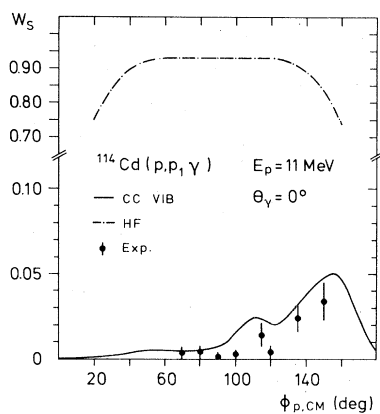


FIG. 7. Experimental spin flip probability of the reaction $^{114}\text{Cd}(p, p_1 \gamma)^{114}\text{Cd}$ in comparison with a Hauser-Feshbach and a coupled channels prediction. (Note the different scale for the compound nucleus and the direct reaction calculation).

(see Table I). The sum over transmission coefficients $\sum T_{ij}$ reflecting the number of open exit channels was replaced by the well-known expression²⁵

$$\sum T_{ij} = 2\pi \frac{\Gamma_0}{D_0} (2J+1) \exp[-J(J+1)/2\sigma^2]. \quad (10)$$

The factor Γ_0/D_0 (Γ_0 and D_0 are the mean level widths and the mean level spacing of the compound nucleus states of the lowest J value to be formed) appearing in the double differential cross sections as well as in the differential cross section cancels in the spin flip probability W_s [cf. Eq. (9)]. For the "spin cutoff" parameter σ we used the value $\sigma = 2.5$. (The spin flip probability W_s is not very sensitive to this parameter. Changing σ from 2.5 to 3.0 gives a variation of W_s of less than 2%.)

Comparing the experimental and theoretical spin flip probability in Fig. 7, it can be seen that the CC calculation assuming a direct reaction alone is able to reproduce the experimental data. Even from small contributions of compound nucleus reactions one would expect considerably higher experimental spin flip probabilities. Therefore, it can be concluded that the compound nucleus contributions are negligible in the reaction $^{114}\text{Cd}(p, p')^{114}\text{Cd}$ at 11 MeV.

COUPLING OF HIGHER STATES

The calculations done in a $0^+ - 2^+$ coupling scheme should reproduce the experimental data of ^{114}Cd in

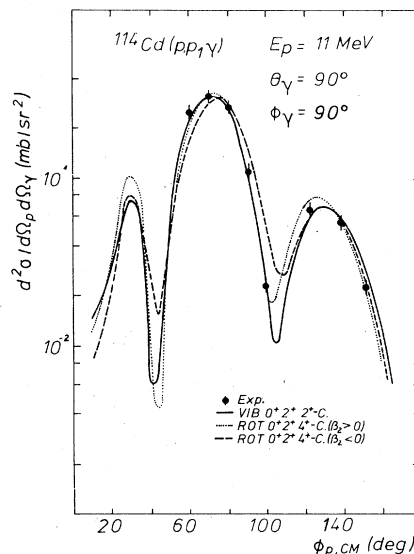


FIG. 8. Experimental double differential cross section of the reaction $^{114}\text{Cd}(p, p_1 \gamma)^{114}\text{Cd}$ in comparison with CC predictions taking into account the coupling of higher states.

a sufficient way, since the influence of coupling higher excited states should be small due to the small coupling strength. Nevertheless, we investigated the effects of coupling higher excited states. The rigid rotator model gives a spin sequence of 0^+ , 2^+ , 4^+ ; therefore, the 4^+ level at 1.282 MeV excitation energy, which decays with a large $B(E2)$ value to the 2^+ level at 558 keV, was taken into account in the CC calculations based on the rotator model. In the case of a vibrational model in which only quadrupole excitations are considered, the spin sequence is 0^+ ; 2^+ ; 0^+ , 2^+ , 4^+ . Actually, for ^{114}Cd one finds two levels with $J^\pi=0^+$ at $E_x=1.133$ MeV and $J^\pi=2^+$ at $E_x=1.208$ MeV, respectively, in addition to the level at $E_x=1.282$ MeV. Both levels decay dominantly to the first excited 2^+ level. We did our calculations in a $0^+-2^+-2^+$ coupling scheme because the 2_2^+ level brings about the strongest excitation in this triplet. Compared with the cal-

culations in a 0^+-2^+ coupling scheme, those coupling higher states show nearly the same results for all measured quantities as expected. In Fig. 8 this is demonstrated for the double differential cross section.

Taking into account all analyses of the present work, it can be concluded that the best description of the experimental data is achieved with the vibrational model. Contributions due to compound reactions are negligible. Although the calculations with the rotational model assuming a prolate deformation cannot reproduce the experimental data as well as the vibrational model, one cannot definitively exclude that model. The rotational model assuming oblate deformation, however, must be ruled out for ^{114}Cd .

We express our thanks to the Erlangen polarized ion source group for their assistance. This work was supported by the Deutsche Forschungsgemeinschaft.

-
- ¹W. Kretschmer and G. Graw, Phys. Rev. Lett. 27, 1294 (1971).
²R. Henneck and G. Graw, Nucl. Phys. A281, 261 (1977).
³J. R. Tesmer and F. H. Schmidt, Phys. Rev. C 5, 864 (1972).
⁴H. Wagner, A. Hofmann, and F. Vogler, Phys. Lett. 47B, 497 (1973).
⁵M. Sakai and T. Tamura, Phys. Lett. 10, 323 (1964).
⁶P. H. Stelson, L. J. C. Ford, Jr., R. L. Robinson, C. Y. Wong, and T. Tamura, Nucl. Phys. A119, 14 (1968).
⁷F. K. McGowan, R. L. Robinson, P. H. Stelson, and J. L. C. Ford, Jr., Nucl. Phys. 66, 97 (1965).
⁸D. Eccleshall, B. M. Hinds, M. J. L. Yates, and N. MacDonald, Nucl. Phys. 37, 377 (1962).
⁹W. Eyrich, A. Hofmann, U. Scheib, S. Schneider, and F. Vogler, Nucl. Instrum. Methods 138, 543 (1976).
¹⁰J. H. Feist, B. Granz, G. Graw, H. Löh, H. Schultz, H. Treiber, in *Proceedings of the Fourth International Symposium on Polarization Phenomena in Nuclear Reactions, Zürich 1975*, edited by W. Grüebler and V. König (Birkhäuser, Basel, 1976) p. 855.
¹¹A. A. Debenham and G. R. Satchler, Particles and Nuclei 3, 117 (1972).
¹²H. H. Barschall and W. Haerberli, *Polarization Phenomena in Nuclear Reactions* (University of Wisconsin Press, Madison, Wisconsin, 1971).
¹³F. Rybicki, T. Tamura, and G. R. Satchler, Nucl. Phys. A146, 659 (1970).
¹⁴T. Tamura, Rev. Mod. Phys. 37, 679 (1965).
¹⁵H. Sherif and J. S. Blair, Phys. Lett. 26B, 489 (1968).
¹⁶J. Raynal, computer code ECIS, CEN Saclay, 1976 (unpublished).
¹⁷U. Scheib (unpublished).
¹⁸H. J. Kim, Nucl. Data Sheets 16, 107 (1975).
¹⁹W. Eyrich, A. Hofmann, U. Scheib, S. Schneider, F. Vogler, and H. Rebel, Phys. Lett. 63B, 406 (1976).
²⁰J. Raynal, in *Proceedings of the Fourth International Symposium on Polarization Phenomena in Nuclear Reactions, Zürich 1975*, edited by W. Grüebler and V. König (Birkhäuser, Basel, 1976), p. 271.
²¹S. Schneider, W. Eyrich, A. Hofmann, U. Scheib, and F. Vogler, Phys. Lett. 80B, 180 (1979).
²²M. Ahmed, J. Lowe, P. M. Rolph, and O. Karban, Nucl. Phys. 147, 273 (1970).
²³W. A. Kolasinski, J. Eenmaa, F. H. Schmidt, H. Sherif, and J. R. Tesmer, Phys. Rev. 180, 1006 (1969).
²⁴E. Sheldon, S. Mathur, and D. Donati, Comp. Phys. Commun. 2, 272 (1971).
²⁵K. A. Eberhard, P. von Brentano, M. Böhning, and R. O. Stephen, Nucl. Phys. A125, 673 (1969).